Structural Snapshots of a Dynamic Coordination Sphere in Model Complexes for Catechol 1,2-Dioxygenases

Michael Merkel,[a] David Schnieders,[a] Sascha M. Baldeau,[a] and Bernt Krebs*[a]

Keywords: Iron / Tripodal ligands / Coordination modes / Enzymes

A series of mononuclear iron(III) complexes as models for intradiol cleaving catechol dioxygenases has been synthesized. In all six compounds, the iron(III) core is coordinated by the ligand [(6-bromo-2-pyridyl)methyl]bis[(2-pyridyl)methyl]amine (brtpa) which mimics the endogenous ligands of this enzyme class and their dynamic behavior. Its steric hindrance pushes the α-substituted pyridine arm of the ligand away from the coordination site in the presence of nucleophiles. This effect turns the iron-brtpa system into an excellent model system for the first step in the reaction mechanism of intradiol cleaving chatechol dioxygenases. The proton acceptor abilities of the bromopyridyl arm are underlined by a hydrogen bond to a coordinated methanol molecule in one of the new compounds and by base dependent kinetic investigations. The presented model system is an effective catalyst that requires between 0.5 and 1.0 fewer equivalents of external base than most other complexes due to the integration of an internal base.

Introduction

The metabolism of aromatic compounds by aerobic bacteria plays an important role in the global carbon cycle.[1,2] Catechol dioxygenases are mononuclear non-heme iron enzymes that can be isolated from bacteria. They catalyze the insertion of dioxygen into catechols with simultaneous ring cleavage. With regards to their regioselectivity they are divided into two major subgroups namely the intradiol and the extradiol cleaving enzymes.[3,4] Protocatechuate 3,4-dioxygenase (3,4-PCD) belongs to the class of intradiol cleaving catechol dioxygenases which catalyze the incorporation of dioxygen into catechols yielding derivatives of *cis,cis*-muconic acid. The X-ray crystal structure of this metalloenzyme reveals a trigonal bipyramidal geometry around the iron(III) core.[5,6] The first ligand sphere consists of two histidines and two tyrosines as endogenous protein ligands (His460, His462, Tyr408, Tyr447) and one solvent derived hydroxide ligand. Spectroscopic and electronic structure studies confirm that the axial Tyr447-Fe^{III} bond is weaker than the equatorial tyrosinate-iron(III) bond.[7]

The interaction of a substrate with Fe^{3+} causes the dissociation of the axial tyrosine and the hydroxide ligand leading to a substrate-iron(III) complex that is best described as octahedral with a vacant site (see Figure 1).[8,9] The departing ligands are believed to act as proton acceptors resulting in a dianionic coordination of the substrate. This enhances its ketonization, yielding a transient carbanion or Fe^{II}-semiquinone radical. The subsequent reaction with O_2 yields a peroxy intermediate which is coordinated to the iron through the remaining open coordination site. Decomposition of this peroxy adduct by a Criegee-type rearrangement affords muconic anhydride.

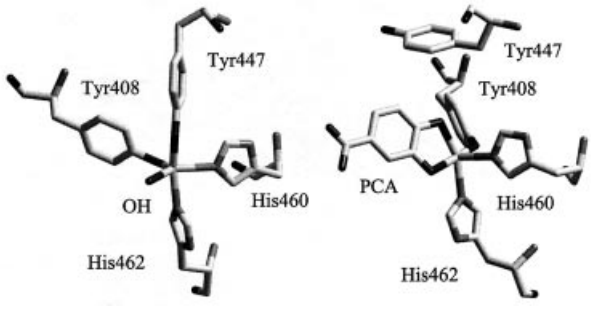

Figure 1. Active site of 3,4-PCD with hydroxide (left) and substrate (right)

In previous studies several functional models have been synthesized in order to gain insight in to the mechanism of catechol cleavage.[10] Whereas in models containing macrocyclic ligands no ligand exchange was observed,[11,12] partial substitutions were reported for coordinated tripodal ligands.[13] Herein we describe 6 crystal structures as well as functional investigations that demonstrate a weak bonding of the substituted arm of [(6-bromo-2-pyridyl)methyl]bis[(2-pyridyl)methyl]amine (brtpa) in iron complexes. The ability to act as an internal base and the replacement of the

[a] Institut für Anorganische und Analytische Chemie der Westfälischen Wilhelms-Universität,
Wilhelm-Klemm-Straße 8, 48149 Münster, Germany
Fax: (internat.) + 49-251-8338366
E-mail: krebs@uni-muenster.de

bromo-substituted pyridine arm by other ligands makes it an excellent functional model for Tyr447 in the enzyme.

Results and Discussion

We were able to characterize six new iron(III) coordination compounds containing the ligand brtpa. In five of these complexes tetrachlorocatecholate (tcc) or tetrabromocatecholate (tbc) was used as a substrate analog, respectively. These catecholates yield compounds that are good structural models for the substrate bound active site of the enzyme and that are not sensitive to air.[14−17]

$[Fe^{III}(brtpa)Br_3]$ (1)

The unit cell of compound **1** consists of four complex molecules, the structure of one such molecule is shown in Figure 2. The structure of **1** is closely related to that of $[Fe^{III}(brtpa)Cl_3]$ reported by Mandon et al.[18] The distorted octahedral coordination sphere of the iron(III) core is composed of three bromide ions and the brtpa ligand. The substituted pyridine does not coordinate, resulting in a tridentate facial coordination mode of the ligand. The three Fe−Br bonds are almost identical [2.447(1), 2.446(1), and 2.441(1) Å] and, as expected, significantly longer than the Fe−Cl bonds in the complex reported by Mandon et al. With respect to the nature of the N donor moieties, the largest Fe−N bond length with a value of 2.298(4) Å occurs between Fe(1) and the tertiary amine nitrogen N(1). Due to their ability to act as π-donors the distances between the nitrogens of the coordinated pyridines and the iron core are significantly shorter [2.197(4) Å and 2.183(4) Å].

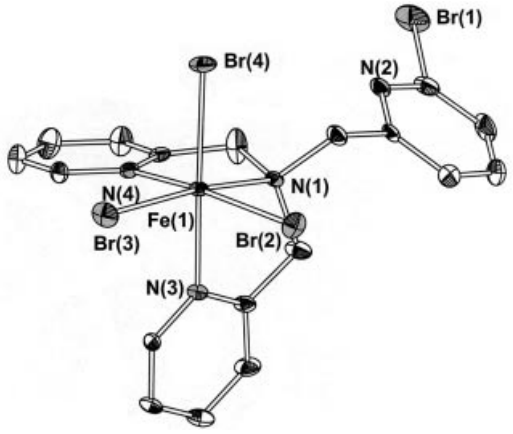

Figure 2. Ellipsoid plot of $[Fe^{III}(brtpa)Br_3]$ (50 % probability); hydrogen atoms omitted for clarity

The existence of five-membered chelate rings causes a distortion of the octahedron towards the tertiary amino group. This is reflected in the low values of the N−Fe−N angles [76.4(2) to 79.8(2)°]. Consequently the angles between the three bromide ligands are expanded [96.1(1) to 99.8(1)°].

$[Fe^{III}(brtpa)(tbc)]ClO_4·H_2O$ (2)

The monoclinic unit cell of compound **2** contains four complex cations, four disordered perchlorates and four water molecules. In contrast to Mandon's $[Fe(brtpa)Cl_3]$ complex[18] and the other iron complexes in this work, compound **2** is the first example of an iron(III) complex in which the brtpa ligand exhibits a tetradentate coordination mode. The remaining coordination sites are occupied by a tetrabromocatecholate dianion (tbc) resulting in a disordered octahedral coordination sphere (Figure 3).

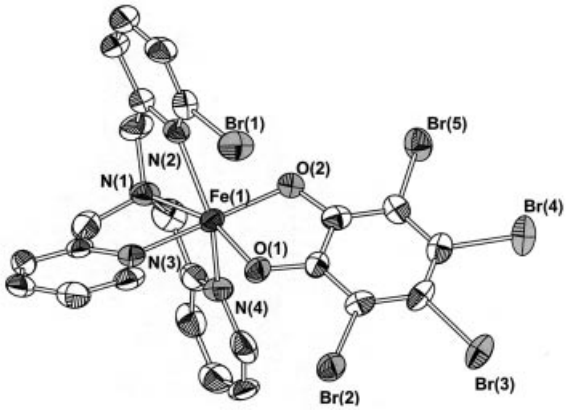

Figure 3. Ellipsoid plot of $[Fe^{III}(brtpa)(tbc)]^+$ (50 % probability); hydrogen atoms omitted for clarity

The similarity of the Fe−O bond lengths [Fe−O(1) = 1.941(5) Å and Fe−O(2) = 1.945(5) Å] demonstrates that the inhibitor substrate coordinates as a dianion rather than a semiquinone. The length of the Fe−N(2) bond [2.220(6) Å] which is the largest Fe−N distance in this complex indicates the weakness of this interaction. The character of this bond originates from the steric demand of the bromo substituent. As a result of this, the O(1)−Fe−N(2) angle is widened to 119.0(2)° which is the largest deviation from the ideal 90° angle and has two effects on the coordination of the catecholate. The first is a twist of 17.8° between the two planes through Fe, N(1), N(3) and Fe, O(1), O(2). Secondly the catecholate is bent down by 12.0° around the O(1)−O(2) axis (see Figure 4). Once again the preorganized five-membered chelate rings of the ligand lead to a significant contraction of the corresponding bond angles.

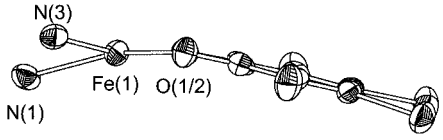

Figure 4. Ellipsoid plot of the catecholate binding in $[Fe^{III}(brtpa)(tbc)]^+$ (50 % probability)

$[Fe^{III}(brtpa)(tcc)(CH_3OH)]ClO_4·CH_3OH$ (3)

Four complex cations, four disordered perchlorate anions and four solvent molecules (methanol) form the unit cell of compound **3**. The iron(III) core is surrounded by the inhibitor substrate tetrachlorocatecholate (tcc), one methanol

molecule and brtpa which coordinates as a tridentate meridional ligand. The bromo-substituted ligand arm has been displaced by the methanol molecule but participates in an intramolecular hydrogen bond with the proton of the coordinated alcohol function. Thus N(2) is tied at a distance of 2.675(6) Å from O(3) and 3.650(4) Å from the iron core. Although methanol is not a particularly good ligand, hydrogen bonds seem to stabilize its coordination to metal centers.[19] Similar intramolecular hydrogen bonds between metal bound solvent molecules and pyridyl moieties have been reported for copper(II) complexes[20,21] and recently for an iron(III) complex.[22] The Fe−O(3) distance of 2.050(4) Å indicates a weaker Fe−O bond compared with the anionic Fe−O_{tcc} interaction [1.924(3) Å and 1.975(4) Å]. The difference in the Fe−O_{tcc} bonds is a consequence of the *trans* effect of the opposing amine nitrogen and oxygen [O(3)] donors.

Due to the limited bite of five-membered chelate rings, the complex cation in **3** reflects the typical distortion of the octahedral coordination sphere. N(1)−Fe−N(3) [77.2(2)°], N(1)−Fe−N(4) [76.6(2)°], and O(1)−Fe−O(2) [83.3(2)°] are reduced, whereas O(1)−Fe−N(3) [97.8(2)°] and O(1)−Fe−N(4) [108.8(2)°] are widened (Figure 5).

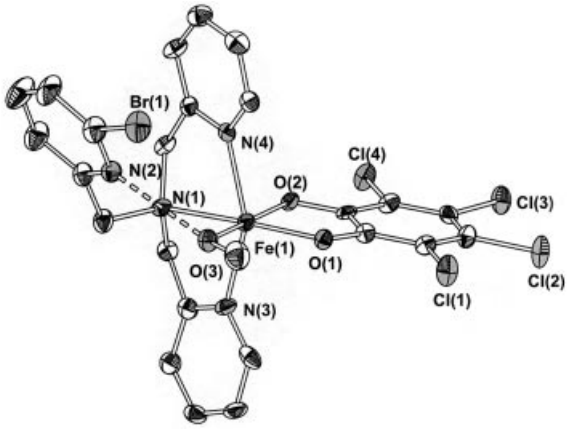

Figure 5. Ellipsoid plot of $[Fe^{III}(brtpa)(tcc)(CH_3OH)]^+$ (50 % probability); hydrogen atoms omitted for clarity

$[Fe^{III}(brtpa)(tcc)Cl]$ (4)

The monoclinic unit cell of compound **4** contains four complex molecules. As in compound **1** the brtpa ligand coordinates in a tridentate facial fashion. The equatorial plane of the octahedron is occupied by the two unsubstituted pyridine arms and the tcc dianion, whereas the axial positions are occupied by the tertiary amine nitrogen and a chloride ligand. As expected, the Fe−N(1) bond is the longest Fe−N bond in this complex [2.337(3) Å]. The slight difference in the Fe−O_{tcc} distance is caused by the asymmetry of the ligand's coordination. The N(1)−C(1) bond is almost in an eclipsed position towards the Fe(1)−O(2) bond, while the Fe(1)−O(1) bond is staggered between N(1)−C(1) and N(1)−C(7). This asymmetry also results in different O(1)−Fe−N(1) and O(2)−Fe−N(1) angles with values of 86.0(2) and 96.7(2)°, respectively. The non coordinating nitrogen atom N(2) of the bromo-substituted ligand arm lies at a distance of 5.278(4) Å from the iron core in this complex (Figure 6).

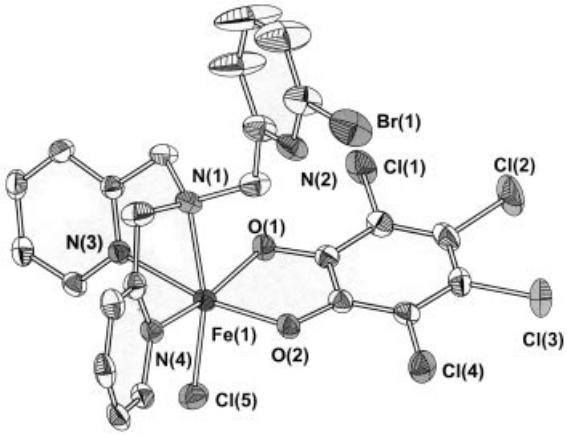

Figure 6. Ellipsoid plot of $[Fe^{III}(brtpa)(tcc)Cl]$ (50 % probability); hydrogen atoms omitted for clarity

$[Fe^{III}(brtpa)(tcc)NO_3]$ (5), $[Fe^{III}(brtpa)(tbc)NO_3]$ (6)

The crystal structures of compounds **5** and **6** show large resemblances to each other. In each of them the unit cell is composed of four iron(III) complexes. The brtpa ligand coordinates in a tridentate facial fashion with its two unsubstituted pyridine units. A nitrate anion and a dianionic catecholate (tcc in **5**; tbc in **6**) complete the octahedral coordination sphere.

The slight difference of 0.02 Å (**5**) and 0.03 Å (**6**) in the iron-catecholate bond lengths is a consequence of the orientation of the non-coordinating bromopyridine arm. This part of the ligand is orientated towards O(2) and thus the O(2)−Fe−N(1) angle is about 12° larger than O(1)−Fe−N(1) in both compounds. Characteristic for tripodal ligands are the long Fe−N(1) distances of 2.260(3) Å (**5**) and 2.252(4) Å (**6**), respectively, and the small angles along the five-membered chelate rings with values of less than 80°.

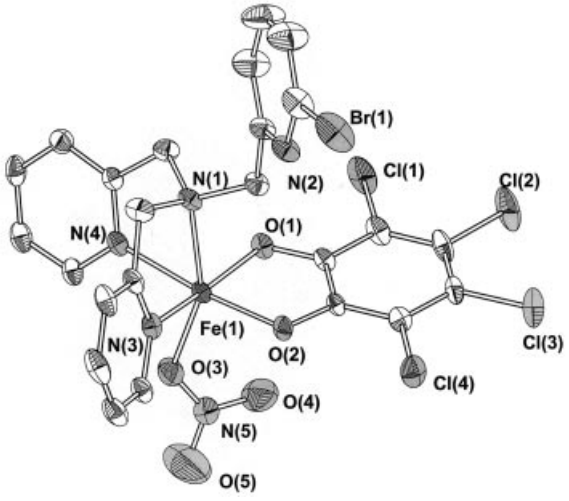

Figure 7. Ellipsoid plot of $[Fe^{III}(brtpa)(tcc)NO_3]$ (50 % probability); hydrogen atoms omitted for clarity

Table 1. Selected bond lengths [Å] and angles [°] in **1**−**6**

1					
Fe(1)−Br(2)	2.447(1)	Br(2)−Fe(1)−Br(3)	96.1(1)	Br(3)−Fe(1)−N(4)	95.0(1)
Fe(1)−Br(3)	2.446(1)	Br(2)−Fe(1)−Br(4)	99.8(1)	Br(4)−Fe(1)−N(1)	90.9(1)
Fe(1)−Br(4)	2.441(1)	Br(2)−Fe(1)−N(1)	90.0(1)	Br(4)−Fe(1)−N(3)	164.3(1)
Fe(1)−N(1)	2.298(4)	Br(2)−Fe(1)−N(3)	89.5(1)	Br(4)−Fe(1)−N(4)	88.6(1)
Fe(1)−N(3)	2.197(4)	Br(2)−Fe(1)−N(4)	165.1(1)	N(1)−Fe(1)−N(3)	76.4(2)
Fe(1)−N(4)	2.183(4)	Br(3)−Fe(1)−Br(4)	97.4(1)	N(1)−Fe(1)−N(4)	77.5(2)
		Br(3)−Fe(1)−N(1)	168.7(1)	N(3)−Fe(1)−N(4)	79.8(2)
		Br(3)−Fe(1)−N(3)	94.1(1)		
2					
Fe(1)−O(1)	1.941(5)	O(1)−Fe(1)−O(2)	83.2(2)	O(2)−Fe(1)−N(4)	94.9(2)
Fe(1)−O(2)	1.945(5)	O(1)−Fe(1)−N(1)	160.7(2)	N(1)−Fe(1)−N(2)	75.4(2)
Fe(1)−N(1)	2.206(7)	O(1)−Fe(1)−N(2)	119.0(2)	N(1)−Fe(1)−N(3)	80.5(3)
Fe(1)−N(2)	2.220(6)	O(1)−Fe(1)−N(3)	87.7(2)	N(1)−Fe(1)−N(4)	75.4(3)
Fe(1)−N(3)	2.113(6)	O(1)−Fe(1)−N(4)	90.5(2)	N(2)−Fe(1)−N(3)	84.7(2)
Fe(1)−N(4)	2.150(7)	O(2)−Fe(1)−N(1)	110.7(2)	N(2)−Fe(1)−N(4)	150.4(3)
		O(2)−Fe(1)−N(2)	91.2(2)	N(3)−Fe(1)−N(4)	94.9(2)
		O(2)−Fe(1)−N(3)	166.7(2)		
3					
Fe(1)−O(1)	1.924(3)	O(1)−Fe(1)−O(2)	83.3(2)	O(2)−Fe(1)−N(4)	90.7(2)
Fe(1)−O(2)	1.975(4)	O(1)−Fe(1)−O(3)	91.7(2)	O(3)−Fe(1)−N(1)	97.0(2)
Fe(1)−O(3)	2.050(4)	O(1)−Fe(1)−N(1)	170.0(2)	O(3)−Fe(1)−N(3)	91.0(2)
Fe(1)−N(1)	2.245(4)	O(1)−Fe(1)−N(3)	97.8(2)	O(3)−Fe(1)−N(4)	87.7(2)
Fe(1)−N(3)	2.094(5)	O(1)−Fe(1)−N(4)	108.8(2)	N(1)−Fe(1)−N(3)	77.2(2)
Fe(1)−N(4)	2.108(4)	O(2)−Fe(1)−O(3)	173.9(2)	N(1)−Fe(1)−N(4)	76.6(2)
Fe(1)−N(2)	3.650(4)	O(2)−Fe(1)−N(1)	88.3(2)	N(3)−Fe(1)−N(4)	153.4(2)
O(3)−N(2)	2.675(6)	O(2)−Fe(1)−N(3)	93.1(2)		
4					
Fe(1)−Cl(5)	2.310(2)	Cl(5)−Fe(1)−O(1)	101.7(1)	O(1)−Fe(1)−N(4)	159.1(2)
Fe(1)−O(1)	1.954(3)	Cl(5)−Fe(1)−O(2)	95.4(1)	O(2)−Fe(1)−N(1)	96.7(2)
Fe(1)−O(2)	1.967(3)	Cl(5)−Fe(1)−N(1)	166.3(1)	O(2)−Fe(1)−N(3)	169.1(2)
Fe(1)−N(1)	2.337(3)	Cl(5)−Fe(1)−N(3)	94.4(1)	O(2)−Fe(1)−N(4)	89.0(2)
Fe(1)−N(3)	2.142(3)	Cl(5)−Fe(1)−N(4)	98.3(1)	N(1)−Fe(1)−N(3)	74.1(2)
Fe(1)−N(4)	2.141(3)	O(1)−Fe(1)−O(2)	83.1(2)	N(1)−Fe(1)−N(4)	75.6(2)
Fe(1)−N(2)	5.278(4)	O(1)−Fe(1)−N(1)	86.0(2)	N(3)−Fe(1)−N(4)	94.1(2)
		O(1)−Fe(1)−N(3)	90.4(2)		
5					
Fe(1)−O(1)	1.946(3)	O(1)−Fe(1)−O(2)	82.9(2)	O(2)−Fe(1)−N(4)	173.8(2)
Fe(1)−O(2)	1.967(3)	O(1)−Fe(1)−O(3)	107.2(2)	O(3)−Fe(1)−N(1)	155.8(2)
Fe(1)−O(3)	1.999(3)	O(1)−Fe(1)−N(1)	89.1(2)	O(3)−Fe(1)−N(3)	89.6(2)
Fe(1)−N(1)	2.260(3)	O(1)−Fe(1)−N(3)	161.9(2)	O(3)−Fe(1)−N(4)	85.7(2)
Fe(1)−N(3)	2.118(4)	O(1)−Fe(1)−N(4)	92.1(2)	N(1)−Fe(1)−N(3)	77.5(2)
Fe(1)−N(4)	2.146(4)	O(2)−Fe(1)−O(3)	99.1(2)	N(1)−Fe(1)−N(4)	75.6(2)
		O(2)−Fe(1)−N(1)	100.7(2)	N(3)−Fe(1)−N(4)	96.2(2)
		O(2)−Fe(1)−N(3)	87.7(2)		
6					
Fe(1)−O(1)	1.940(3)	O(1)−Fe(1)−O(2)	82.9(2)	O(2)−Fe(1)−N(4)	173.3(2)
Fe(1)−O(2)	1.970(3)	O(1)−Fe(1)−O(3)	107.7(2)	O(3)−Fe(1)−N(1)	155.5(2)
Fe(1)−O(3)	1.991(3)	O(1)−Fe(1)−N(1)	88.6(2)	O(3)−Fe(1)−N(3)	89.5(2)
Fe(1)−N(1)	2.252(4)	O(1)−Fe(1)−N(3)	161.9(2)	O(3)−Fe(1)−N(4)	85.6(2)
Fe(1)−N(3)	2.131(3)	O(1)−Fe(1)−N(4)	91.2(2)	N(1)−Fe(1)−N(3)	77.2(2)
Fe(1)−N(4)	2.146(4)	O(2)−Fe(1)−O(3)	99.0(2)	N(1)−Fe(1)−N(4)	75.6(2)
		O(2)−Fe(1)−N(1)	101.2(2)	N(3)−Fe(1)−N(4)	96.0(2)
		O(2)−Fe(1)−N(3)	88.9(2)		

The large resemblances of **5** and **6** demonstrate that it is legitimate to compare compounds **2**, **3**, and **4** even though different inhibitor substrates are involved. As a representative of the two isostructural compounds the crystal structure of **5** is shown in Figure 7.

Selected bond lengths and angles for the iron(III) complexes are reported in Table 1.

Oxygenation of Bonded dbc in the Presence of Dioxygen

Stoichiometric Kinetic Studies

In order to gain information on the catechol cleavage activity, the decrease in the lower energy LMCT band was

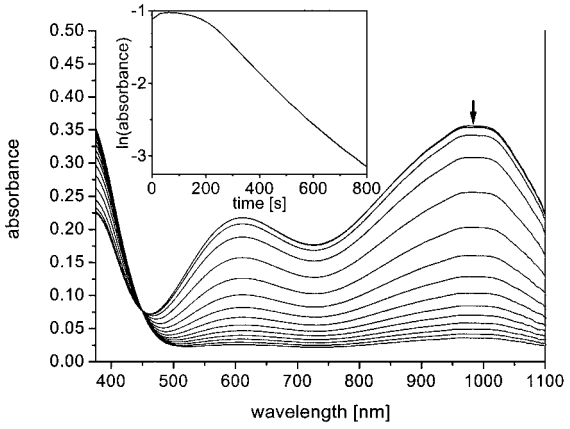

Figure 8. Progress of the reaction of $[Fe^{III}(brtpa)(dbc)]^+$ with dioxygen; inset: plot of ln(absorption)vs. time for this reaction (ambient temperature; 1.5 equiv. of base)

monitored by UV/Vis-spectroscopy. Figure 8 shows the decrease of this band during the reaction of in situ prepared $[Fe(brtpa)(dbc)]^+$ (where dbc = 3,5-di-*tert*-butylcatecholate) with dioxygen which is present in methanol saturated with air. A greater than tenfold excess of dioxygen ensures pseudo-first-order kinetics for the complete reaction and therefore a linear dependency of the plot of ln(absorbance) vs. time (inset in Figure 8) can be observed. By considering the concentration of dioxygen in air saturated methanol at ambient temperature, the reaction rate constant k can be obtained from the slope of this linear graph.

Different amounts of piperidine were added to the reaction mixture to ensure a dianionic binding of the substrate and thus a high reactivity. As can be seen from Figure 9, the highest reactivity was reached when 1.5 equivalents of base were added to the reaction mixture. Although complexes derived from similar tripodal ligands show catechol dioxygenase activity under the same conditions the highest activity can be observed upon addition of 2.0−2.5 equivalents of base in these systems.[14,16] The lower demand of base in the reaction of the new model compound can be explained by the peculiarity of the ligand and its weakly coordinated bromopyridine unit. As indicated by the intramolecular hydrogen bond in **3**, this unit can act as a proton acceptor and therefore as an internal base. Furthermore this behavior was confirmed by spectrophotometric titrations of a complex-catechol mixture with piperidine in which only 1.8 equivalents of the base were needed for an optimal dianionic binding of the catechol. The closely related me_1tpa system, where the bromine in brtpa is substituted by a methyl group, needs significantly more (2.4 equiv.) base to bind the catechol.[16]

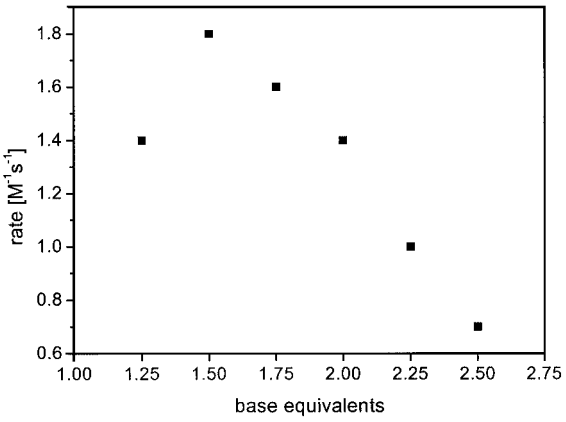

Figure 9. Correlation of reaction rates *k* and added equivalents of piperidine

As shown in Figure 9, a maximum reaction rate of 1.8 $M^{-1}s^{-1}$ was found for the iron brtpa system. This is of the same order of magnitude as those reported for other model compounds containing tripodal ligands. (For review articles see ref.[10])

Taking into consideration that Ogo et al. reported a model system in which coordinated acetylacetonate is used as an internal base,[23] it should be possible to generate the iron(III) complex $[Fe(brtpa)(acac)]^{2+}$ which allows cleavage of catechols without any further addition of base.

Identification of the Cleavage Products

The oxygenated products were characterized by GC/MS as well as ^1H NMR spectroscopy. Neither of these methods showed evidence for the undesired products of simple oxidation (quinones) or extradiol cleavage. The amount of external base in the reaction mixture (1.5 or 2.0 equiv.) had no effect on the product composition. In acetonitrile and dichloromethane, muconic anhydride was found as the exclusive reaction product whereas in methanol a mixture of muconic anhydride and its methanolysis product was detected by GC/MS. All results demonstrate that the present model system exclusively catalyzes the intradiol cleavage reaction.

Catalytic Reactions

The identification of the cleavage products was also performed for catalytic reactions. The substrate-catechol ratio in these experiments was 10:1 and 100:1, respectively. Even for the 100 fold excess of substrate, we observed complete conversion of the catechol. The GC/MS analysis revealed that only the desired intradiol cleavage products were formed in the reaction.

Conclusion

With the crystal structures and functional investigations reported in this work we have established an excellent model system for the first steps in the reaction mechanism of catechol dioxygenases. The substituted pyridine moiety is a good mimic for the departing tyrosine ligand in the enzyme. This was demonstrated by the different positions of the ligand arm resulting in an increase of the corresponding Fe−N distance from 2.22 to 5.28 Å. Furthermore, the base dependent kinetic investigations revealed that the bromopyridine arm acts as an internal base. This behavior is confirmed by the presence of a hydrogen bond in **3**.

Experimental Section

Materials: All chemicals were purchased from commercial sources and used without any further purification.

Physical Measurements: ^{1}H and ^{13}C NMR spectra were measured on a Bruker WH 300 spectrometer. UV/Vis spectroscopy was performed on a Hewlett−Packard 8453 diode array spectrometer.

Syntheses

[(6-Bromo-2-pyridyl)methyl][(2-pyridyl)methyl]amine (brbpa): 6-Bromo-2-pyridine carboxaldehyde (20.0 g, 107.5 mmol) was stirred in methanol (100 mL). After slow addition of 2-(aminomethyl)pyridine (11.6 g, 107.5 mmol, 11.2 mL) the solution was stirred for a further 2 h. At 0 °C sodium borohydride (3.0 g, 79.3 mmol) was carefully added. The reaction mixture was stirred overnight and allowed to warm to room temperature. The mixture was acidified with hydrochloric acid to pH 1 and extracted with chloroform (5 × 40 mL) to separate impurities and side products. In order to neutralize the hydrochloride, the pH was adjusted to 8 with an aqueous solution of sodium hydroxide and the free amine was extracted with chloroform (5 × 40 mL). The combined organic layers were dried over $MgSO_4$ and the solvent was removed in vacuo yielding 24.62 g (88.5 mmol; 82 %) of a yellow oil which was used without further purification. ^{1}H NMR (400 MHz, $CDCl_3$): δ = 3.95 (s, 2 H, CH_2), 3.96 (s, 2 H, CH_2), 7.16 (m, 1 H, CH), 7.33 (m, 3 H, CH), 7.45 (t, 1 H, CH), 7.60 (m, 1 H, CH), 8.54 (d, 1 H, CH) ppm. ^{13}C NMR (100 MHz, $CDCl_3$): δ = 54.3, 54.7, 121.0, 122.0, 122.3, 126.2, 136.4, 138.8, 141.7, 149.4 159.6, 161.8.

[(6-Bromo-2-pyridyl)methyl]bis[(2-pyridyl)methyl]amine (brtpa): To a stirred mixture of brbpa (14.33 g, 51.5 mmol) and 2-picolyl chloride hydrochloride (8.45 g, 51.5 mmol) in THF (100 mL) was added triethylamine (14.4 mL, 10.5 g, 103 mmol). After heating to reflux for 48 h the mixture was cooled to room temperature and the resultant precipitate removed by filtration. The red solution was concentrated in vacuo. The residual red oil was extracted with boiling diethyl ether and upon cooling to −18 °C the off-white product precipitated. Yield 13.69 g (37.1 mmol; 72 %). NMR spectroscopic data have already been published.[24]

[Fe^{III}(brtpa)Br$_3$] (1): Iron(III) bromide (30 mg; 0.1 mmol) and brtpa (37 mg; 0.1 mmol) were stirred in acetone/methanol (6 mL, 1:1 mixture) for a few minutes. The mixture was then heated to reflux for a few seconds and filtered. Red crystals of complex **1** formed

Table 2. Crystallographic data and experimental details {$w = 1/[\sigma^2(F_o^2) + (xP)^2 + 0P]$, $P = (F_o^2 + 2F_c^2)/3$; **1**: $x = 0.0993$; **2**: $x = 0.0660$; **3**: $x = 0.0643$; **4**: $x = 0.0607$; **5**: $x = 0.1473$; **6**: $x = 0.0493$}

Compound	**1**	**2**	**3**	**4**	**5**	**6**
Empirical formula	$C_{18}H_{17}Br_4FeN_4$	$C_{24}H_{19}Br_5ClFeN_4O_7$	$C_{26}H_{25}BrCl_5FeN_4O_8$	$C_{24}H_{17}BrCl_5FeN_4O_2$	$C_{24}H_{17}BrCl_4FeN_5O_5$	$C_{24}H_{17}Br_5FeN_5O_5$
M_r	664.85	966.26	834.51	706.43	732.99	910.83
Temperature [K]	200(2)	100(2)	100(2)	183(2)	200(2)	193(2)
Radiation (λ [Å])	Cu-K_α (1.54178)	Cu-K_α (1.54178)	Cu-K_α (1.54178)	Cu-K_α (1.54178)	Cu-K_α (1.54178)	Cu-K_α (1.54178)
Crystal shape	red plate	dark blue rod	dark blue rod	red plate	red plate	red rod
Crystal size [mm]	0.32 × 0.15 × 0.05	0.34 × 0.12 × 0.09	0.29 × 0.08 × 0.08	0.30 × 0.20 × 0.20	0.45 × 0.34 × 0.10	0.35 × 0.11 × 0.06
Crystal system	monoclinic	monoclinic	monoclinic	monoclinic	monoclinic	monoclinic
Space group	$P2_1/c$ (No. 14)	$P2_1/c$ (No. 14)	$P2_1/n$ (No. 14)	$P2_1/n$ (No. 14)	$P2_1/n$ (No. 14)	$P2_1/n$ (No. 14)
a [Å]	7.42730(10)	19.6180(5)	8.4029(3)	11.9632(2)	12.1670(1)	12.4211(1)
b [Å]	19.4257(2)	9.1403(3)	19.6182(5)	15.5977(2)	15.3780(2)	15.5936(2)
c [Å]	14.86490(10)	17.4979(5)	19.1890(5)	15.1630(2)	15.2474(2)	15.4273(2)
β [°]	96.3360(10)	108.688(2)	95.286(2)	110.780(1)	107.089(1)	108.670(1)
V [Å^3]	2131.61(4)	2972.20(15)	3149.85(16)	2645.34(7)	2726.90(6)	2830.87(6)
Z	4	4	4	4	4	4
$\rho_{calcd.}$ [g·cm^{-3}]	2.072	2.155	1.760	1.774	1.785	2.137
μ [mm^{-1}]	14.547	13.220	9.712	11.260	10.167	12.936
F(000)	1276	1852	1676	1404	1460	1748
Scan range θ [°]	3.76 to 71.42	2.38 to 71.22	3.23 to 71.33	4.07 to 71.17	4.11 to 71.64	4.00 to 71.13
Index ranges	$-9 \le h \le 7$	$-21 \le h \le 23$	$-9 \le h \le 10$	$-14 \le h \le 13$	$-14 \le h \le 14$	$-13 \le h \le 14$
	$-23 \le k \le 23$	$-9 \le k \le 11$	$-22 \le k \le 23$	$-19 \le k \le 16$	$-18 \le k \le 17$	$-18 \le k \le 19$
	$-16 \le l \le 17$	$-21 \le l \le 21$	$-23 \le l \le 23$	$-18 \le l \le 15$	$-18 \le l \le 17$	$-18 \le l \le 17$
Reflections collected	12272	16319	17671	14982	15646	16001
Unique reflections	3994	5196	5820	4486	5046	5272
Reflections $I > 2\sigma(I)$	3668	3302	3712	3397	4264	4085
R_{int}	0.0793	0.0765	0.0708	0.0551	0.1187	0.0633
Data/restraints/parameters	3994/0/244	5196/0/398	5820/0/427	4486/0/334	5046/0/361	5272/0/371
Goodness-of-fit on F^2	1.032	0.966	0.952	0.984	1.032	0.944
Final R indices [$I > 2\sigma(I)$]	$R1 = 0.0491$	$R1 = 0.0533$	$R1 = 0.0554$	$R1 = 0.0425$	$R1 = 0.0708$	$R1 = 0.0395$
	$wR2 = 0.1312$	$wR2 = 0.1269$	$wR2 = 0.1280$	$wR2 = 0.1083$	$wR2 = 0.1885$	$wR2 = 0.0919$
R indices (all data)	$R1 = 0.0518$	$R1 = 0.0865$	$R1 = 0.0884$	$R1 = 0.0550$	$R1 = 0.0784$	$R1 = 0.0512$
	$wR2 = 0.1335$	$wR2 = 0.1373$	$wR2 = 0.1378$	$wR2 = 0.1126$	$wR2 = 0.1958$	$wR2 = 0.0957$
Largest diff. peak/hole [e·Å^{-3}]	1.138/−1.345	1.028/−1.095	0.790/−0.790	0.557/−0.639	1.015/−1.507	0.511/−1.108

upon slow cooling. $C_{18}H_{17}Br_4FeN_4$ (664.82 g/mol). Crystal data are given in Table 2.

[Fe^{III}(brtpa)(tbc)]ClO_4·H_2O (2): To a stirred solution of iron(III) perchlorate hydrate (37 mg; 0.1 mmol) and brtpa (37 mg; 0.1 mmol) in of acetone (7 mL) was added tetrabromocatechol (42 mg; 0.1 mmol). After addition of triethylamine (20 mg, 28 μL, 0.2 mmol) the mixture was stirred for a few minutes and filtered. Upon slow diffusion of diethyl ether into the solution dark blue crystals of **2** preciptiated. $C_{24}H_{19}Br_5ClFeN_4O_7$ (966.26 g/mol). Crystal data are given in Table 2.

[Fe^{III}(brtpa)(tcc)(CH_3OH)]ClO_4·CH_3OH (3): $Fe(ClO_4)_3$·H_2O (37 mg; 0.1 mmol) and brtpa (37 mg; 0.1 mmol) were dissolved in methanol/acetone (9 mL, 3:1 mixture). After addition of tetrachlorochatechol monohydrate (26 mg; 0.1 mmol) and triethylamine (28 μL, 20 mg; 0.2 mmol) the mixture was stirred for a few minutes and filtered. Upon slow diffusion of diethyl ether into the solution dark blue crystals of compound **3** precipitated. $C_{26}H_{25}BrCl_5FeN_4O_8$ (834.52 g/mol). Crystal data are given in Table 2.

[Fe^{III}(brtpa)(tcc)Cl] (4): To a stirred solution of $FeCl_3$ (16 mg; 0.1 mmol), brtpa (37 mg; 0.1 mmol) and tetrachlorocatechol monohydrate (26 mg; 0.1 mmol) in methanol/acetone (7 mL, 1:3 mixture) was added triethylamine (20 mg, 28 μL, 0.2 mmol). After heating to reflux for a few seconds the mixture was filtered and slow diffusion of diethyl ether into the solution yielded red plates of complex **4**. $C_{24}H_{17}BrCl_5FeN_4O_2$ (706.44 g/mol). Crystal data are given in Table 2.

[Fe^{III}(brtpa)(tcc)NO_3] (5): To a stirred solution of $Fe(NO_3)_3$·$9H_2O$ (40 mg; 0.1 mmol), brtpa (37 mg; 0.1 mmol) and tetrachlorocatechol monohydrate (26 mg; 0.1 mmol) in methanol/acetone (7 mL, 3:1 mixture) was added triethylamine (20 mg, 28 μL, 0.2 mmol). After heating to reflux for a few seconds the mixture was filtered and slow diffusion of diethyl ether into the solution yielded red crystals of complex **5**. $C_{24}H_{17}Br_5FeN_5O_5$ (910.80 g/mol). Crystal data are given in Table 2.

[Fe^{III}(brtpa)(tbc)NO_3] (6) To a stirred solution of $Fe(NO_3)_3$·$9H_2O$ (40 mg; 0.1 mmol), brtpa (37 mg; 0.1 mmol) and tetrabromocatechol (42 mg; 0.1 mmol) in methanol/acetone (9 mL, 1:1 mixture) was added triethylamine (20 mg, 28 μL, 0.2 mmol). After heating to reflux for a few seconds the mixture was filtered and slow diffusion of diethyl ether into the solution yielded red plates of complex **6**. $C_{24}H_{17}BrCl_4FeN_5O_5$ (732.99 g/mol). Crystal data are given in Table 2.

Stoichiometric Kinetic Studies: The catechol cleavage activity of an in situ prepared complex solution was tested under addition of between 1.0 and 2.5 equivalents of piperidine as an external base. To a $2{\cdot}10^{-4}$ mol·L^{-1} methanolic solution (2 mL) consisting of $Fe(ClO_4)_3$·H_2O and the ligand was added a $2{\cdot}10^{-2}$ mol·L^{-1} (1 equivalent) solution of 3,5-H_2dbc (0.02 mL). The amount of base added to the reaction mixture was varied from 0.02 mL to 0.05 mL (1.0−2.5 equiv.; increment 0.005 mL; 0.25 equiv.) of a $2{\cdot}10^{-2}$ mol·L^{-1} solution. The decomposition of the complexes was followed at least three times by UV/Vis spectroscopy. Spectrophotometric titrations were carried out with the same solutions in a flow cell under an argon atmosphere.

Identification of the Cleavage Products

Stoichiometric Reactions: Identification of the reaction products was also carried out in presence of different amounts of base and in different organic solvents (dichloromethane, acetonitrile and methanol). To a stirred solution of $Fe(ClO_4)$·H_2O, the ligand brtpa and catechol (0.2 mmol) was added 1.5 or 2.0 equivalents of piperidine, respectively. After all catechol had reacted the solvent was evaporated under reduced pressure at ambient temperature. The iron complex was removed by silica gel filtration (CH_2Cl_2/$CHCl_3$, 1:2). After evaporation of the solvent (ambient temperature) the products were dried in vacuo and identified by GC/MS-coupling and ^{1}H NMR spectroscopy.

Catalytic Reactions: The reactions were carried out in acetonitrile solutions. To a stirred complex solution (0.1 and 0.01 mmol dissolved in 50 mL, respectively) were added 3,5-H_2dbc (222.3 mg, 1 mmol) and 1.5 equiv. of piperidine (relative to the iron complex). To ensure fast reactions, dioxygen was bubbled through the reaction mixture. Workup of the oxygenated products was done according to the procedure described for the stoichiometric reactions.

X-ray Crystal Structures

Intensity data of all complexes were collected on a Bruker AXS SMART 6000 CCD diffractometer (Cu-K_α, λ = 1.54178 Å, Göbel mirror) using the ω-scan technique. The collected reflections were corrected for absorption effects.[25] All structures were solved by direct methods and refined by full-matrix least-squares methods on F^2.[26] Further data collection parameters are summarized in Table 2.

CCDC-213838 to -213843 contain the supplementary crystallographic data for this paper. These data can be obtained free of charge at www.ccdc.cam.ac.uk/conts/retrieving.html [or from the Cambridge Crystallographic Data Center, 12, Union Road, Cambridge CB2 1EZ, UK; Fax: (internat.) +44-1223-336-033; E-mail: deposit@ccdc.cam.ac.uk].

Acknowledgments

Financial support from the Deutsche Forschungsgemeinschaft, the Fonds der Chemischen Industrie and the Bundesminsterium für Bildung und Forschung is gratefully acknowledged. M. M. thanks the University of Münster for a graduate fellowship.

[1] L. Que, Jr., R. Y. N. Ho, *Chem. Rev.* **1996**, *96*, 2607.
[2] T. D. H. Bugg, C. J. Winfield, *Nat. Prod. Rep.* **1998**, *15*, 513.
[3] E. F. Elstner, *Der Sauerstoff*, Wissenschaftsverlag, Mannheim, Wien, Zürich, **1990**.
[4] L. Que, Jr., *Bioinorganic Catalysis* (Eds.: J. Reedijk, E. Bouwman), 2nd ed., Marcel Dekker Inc., New York, Basel, **1999**.
[5] D. H. Ohlendorf, J. D. Lipscomb, P. C. Weber, *Nature* **1988**, *336*, 403.
[6] D. H. Ohlendorf, A. M. Orville, J. D. Lipscomb, *J. Mol. Biol.* **1994**, *244*, 586.
[7] M. I. Davis, A. M. Orville, F. Neese, J. M. Zaleski, J. D. Lipscomb, E. I. Solomon, *J. Am. Chem. Soc.* **2002**, *124*, 602.
[8] M. W. Vetting, D. A. D'Argenio, L. N. Ornston, D. H. Ohlendorf, *Biochemistry* **2000**, *39*, 7943.
[9] A. M. Orville, J. D. Lipscomb, D. H. Ohlendorf, *Biochemistry* **1997**, *36*, 10052.
[10] Review Articles: ref.[1]; R. Yamahara, S. Ogo, H. Masuda, Y. Watanabe, *J. Inorg. Biochem.* **2002**, *88*, 284.
[11] W. O. Koch, H.-J. Krüger, *Angew. Chem.* **1995**, *107*, 2928; *Angew. Chem. Int. Ed. Engl.* **1995**, *34*, 2671.
[12] N. Raffard, R. Carina, A. J. Simaan, J. Sainton, E. Rivière, L. Tchertanov, S. Bourcier, G. Bouchoux, M. Delroisse, F. Banse, J.-J. Girerd, *Eur. J. Inorg. Chem.* **2001**, 2249.
[13] R. R. Jacobson, Z. Tyeklar, A. Farooq, K. D. Karlin, S. Liu, J. Zubieta, *J. Am. Chem. Soc.* **1988**, *110*, 3690.

[14] M. Pascaly, M. Duda, A. Rompel, B. H. Sift, W. Meyer-Klaucke, B. Krebs, *Inorg. Chim. Acta* **1999**, *291*, 289.
[15] F. Schweppe, H. Sirges, M. Pascaly, M. Duda, Ç. Nazikkol, W. Steinforth, B. Krebs, *Peroxide Chemistry. Mechanistic and Preparative Aspects of Oxygen Transfer* (Ed.: W. Adam), Wiley VCH, Weinheim, **2000**, 232.
[16] M. Pascaly, M. Duda, F. Schweppe, K. Zurlinden, F. K. Müller, B. Krebs, *J. Chem. Soc., Dalton Trans.* **2001**, 828.
[17] M. Merkel, F. K. Müller, B. Krebs, *Inorg. Chim. Acta* **2002**, *337*, 308.
[18] D. Mandon, A. Nopper, T. Litrol, S. Goetz, *Inorg. Chem.* **2001**, *40*, 4803.
[19] C. J. Boxwell, P. H. Walton, *Chem. Commun.* **1999**, 1647.
[20] S. P. Foxon, O. Walter, S. Schindler, *Eur. J. Inorg. Chem.* **2002**, 111.
[21] J. M. Rowland, M. M. Olmstead, P. K. Mascharak, *Inorg. Chem.* **2000**, *39*, 5326.
[22] S. Zhu, W. W. Brennessel, R. G. Harrison, L. Que, Jr., *Inorg. Chim. Acta*, in press.
[23] R. Yamahara, S. Ogo, Y. Watanabe, T. Funabiki, K. Jitsukawa, H. Masuda, H. Einaga, *Inorg. Chim. Acta* **2000**, *300*, 587.
[24] C.-L. Chuang, O. dos Santos, X. Xu, J. W. Canary, *Inorg. Chem.* **1997**, *36*, 1967.
[25] *Siemens Area Detector Absorption Correction,* Siemens.
[26] G. M. Sheldrick, *SHELX-97*, University of Göttingen, **1997**.

Received July 1, 2003
Early View Article
Published Online December 12, 2003

